JOURNAL OF MATERIALS SCIENCE 41 (2006) 251–258

Properties of triglycine sulfate/poly(vinylidene fluoride-trifluoroethylene) 0-3 composites

Y. YANG, H. L. W. CHAN, C. L. CHOY
Department of Applied Physics and Materials Research Centre, The Hong Kong Polytechnic University, Hung Hom, Kowloon, Hong Kong, China
E-mail: apahlcha@polyu.edu.hk

Composites of triglycine sulfate (TGS) powder dispersed in a poly(vinylidene fluoride-trifluoroethylene) (P(VDF-TrFE), 70/30 mol%) copolymer matrix have been prepared using solvent casting followed by compression moulding. The composites have been characterized by means of scanning electron microscopy (SEM) and differential scanning calorimetry (DSC). Three groups of samples have been prepared: unpoled composites, composites with only the TGS phase poled and composites with both phases poled. The observed relative permittivity of these composites are consistent with the predictions of the Bruggeman model. When the TGS and copolymer phases are poled in the same direction, the piezoelectric activities of the two phases partially cancel each other while the pyroelectric activities reinforce. The pyroelectric coefficients exhibit good agreement with the effective-medium model. These composites have high pyroelectric figures of merit which increase as the volume fraction of TGS increases.

1. Introduction

Ferroelectric ceramic/polymer 0-3 composites have a considerable potential in pyroelectric sensor, ultrasonic transducer and underwater hydrophone applications as they combine high piezoelectric and pyroelectric activities of the ceramic with the mechanical flexibility and low acoustic impedance of the polymer [1–5]. If both the inclusion and the matrix are ferroelectric, the poling state of the matrix provides an additional feature and it is possible to produce composites with only the ceramic poled or with both the ceramic phase and the matrix poled in the same direction [4]. Hence, P(VDF-TrFE) copolymers (with TrFE content >20 mol%) have been chosen as the electroactive matrix in ceramic/polymer 0-3 composites in recent years [3, 4]. In selecting the inclusion, many conventional pyroelectric ceramic materials with high pyroelectric activity and dielectric permittivity have been used, e.g. $PbTiO_3$ [2] and lead zirconate titanate [5].

The main aim of this work is to produce 0-3 composites with high pyroelectric activity and high pyroelectric figures of merit. Based on the effective-medium approach [6], the pyroelectric coefficient p of a composite can be calculated by:

$$p = \left(\frac{\varepsilon - \varepsilon_m}{\varepsilon_i - \varepsilon_m}\right) \cdot p_i + \left(\frac{\varepsilon_i - \varepsilon}{\varepsilon_i - \varepsilon_m}\right) \cdot p_m \qquad (1)$$

where ε, ε_i and ε_m are the relative permittivities of the composite, inclusion and matrix, respectively and p_i and p_m are the pyroelectric coefficients of the inclusion and matrix, respectively. Using this equation, it is found that high relative permittivity of the inclusion will inhibit the improvement of pyroelectric properties in 0-3 composites. Therefore, triglycine sulfate (TGS), which is a well-known pyroelectric crystal having a high pyroelectric coefficient and a low relative permittivity, would be an ideal material to be used as the inclusion phase. Although TGS single crystals have high pyroelectric figures of merit, they are very fragile and water-soluble. These make it difficult to use TGS crystals in pyroelectric devices. In previous publications, studies on TGS/PVDF 0-3 composites have been reported [7, 8]. However, there is no systematic study on TGS/P(VDF-TrFE) 0-3 composites. In this work, the dielectric, piezoelectric and pyroelectric properties of

0022-2461
DOI: 10.1007/s10853-005-7245-1

TGS/P(VDF-TrFE) 0-3 composites are studied in detail.

2. Experimental procedure

2.1. Fabrication of TGS/P(VDF-TrFE) 0-3 composites

The P(VDF-TrFE) 70/30 mol% copolymer used as the matrix phase in the present study was supplied by Piezotech, France. The TGS single crystal and powder were supplied by the Institute of Crystal Materials, Shandong University, China.

Powder of P(VDF-TrFE) 70/30 mol% copolymer was dissolved in dimethylformamide (DMF) and then predetermined amount of TGS powder (size $\sim$5 μm) was dispersed into the solution. After 20 min of ultrasonic agitation, the solution was stirred magnetically at 60°C until a gel-form composite was obtained. In order to remove the solvent completely, the thick composite film was dried at 80°C in a vacuum oven for 12 h. The thick film was then crushed into small pieces and compression moulded at 160°C under a pressure of 15 MPa. After 15 min, the mould was then removed and cooled to room temperature in air. In order to enhance the crystallinity, the composite films were annealed at 130°C for 2 h. The final thickness of the composite film was about 70 μm. Cr-Au electrodes were deposited on both sides of the film for subsequent property measurements. TGS/P(VDF-TrFE) 0-3 composites with various volume fractions of TGS $\phi = 0.05, 0.11, 0.22, 0.27, 0.33$ and 0.43 were fabricated.

2.2. Poling process

To impart piezoelectric and pyroelectric activities to the samples, they were subjected to a poling process so as to orient the dipoles in the TGS and P(VDF-TrFE) phases. In the present study, two groups of samples were poled in an oil bath. In group 1, both phases were poled and in group 2 only the TGS phase was poled. The poling procedures are described as follows:

Group 1: Samples were heated to 70°C and a stepwise poling method was used. Firstly, samples were poled at 70°C with a field of 60 V/μm for 30 min. At this temperature, only the copolymer phase was poled since TGS was in the paraelectric phase (the Curie temperature of TGS is 49°C). Secondly, the field was decreased to 10 V/μm and the sample was cooled from 70°C to ambient temperature in a period of about 1h with the electric field applied. During the cooling process, TGS went through a transition from the paraelectric phase to the ferroelectric phase with the field applied.

Group 2: Samples were heated to 70°C and a field of 10 V/μm was applied. Then the samples were cooled to room temperature with the electric field kept on. The copolymer matrix could not be poled with such a low field. To verify that only the TGS phase was poled, the same procedure was applied to a pure copolymer sample. The copolymer has no detectable piezoelectric or pyroelectric activities, thus showing that it was not polarized.

2.3. Characterization

Three series of composites were prepared for characterization: unpoled composites, composites with only the TGS phase poled and composites with both phases poled. The structure, phase transitions and dielectric, piezoelectric and pyroelectric properties of the composites were investigated. The microstructure of TGS/P(VDF-TrFE) 0-3 composites was observed using a scanning electron microscope (JEOL JSM-6335F FE-SEM). Thermal measurements were performed with a differential scanning calorimeter (Perkin-Elmer DSC7). The heating or cooling rate was 10°C/min in the temperature range of -20 to 130°C. The relative permittivity ε_r and loss factor tan δ as a function of temperature from -20 to 120°C at 10 kHz were determined using an impedance analyzer (HP 4194A) equipped with a temperature chamber (Delta 9023). The relative permittivity ε_r and loss factor tan δ as a function of frequency from 1 kHz to 10 MHz were also measured at room temperature (about 22°C). The piezoelectric coefficient d_{33} of the composites was measured using a piezo d_{33} meter (Model ZJ-3D, Beijing Institute of Acoustics, China). A sinusoidal mechanical stress with a frequency of 60 Hz was applied to the sample while the current signal was recorded. The pyroelectric coefficient p was measured using a dynamic method [9]. At a certain temperature T the sample temperature was sinusoidally modulated [$T(t) = T + T_\sim \sin 2\pi ft$] with frequency $f =$ 55 mHz and amplitude $T_\sim = 1$K using a Peltier element. The pyroelectric current signal was amplified with an electrometer and the 90° out of phase component of the current with respect to the temperature modulation was measured with a lock-in amplifier.

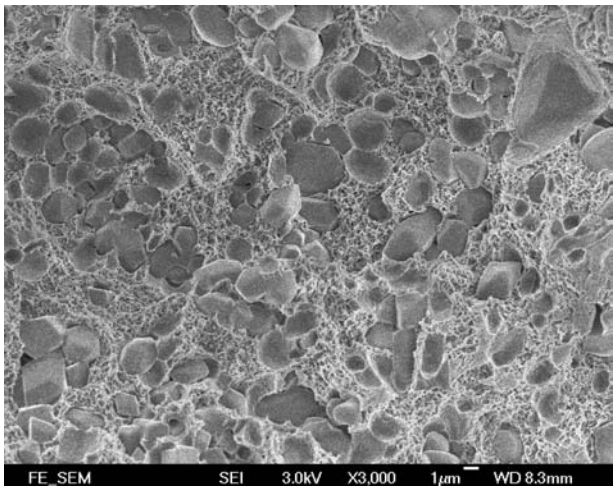

Figure 1 SEM micrograph of the fracture surface for TGS/P(VDF-TrFE) 0-3 composite with $\phi = 0.43$.

3. Results and discussion

3.1. Microstructures

The cross-sectional micrograph of the composite with $\phi = 0.43$ is shown in Fig. 1. It is seen that the TGS particles are dispersed rather uniformly in the copolymer matrix.

3.2. Phase transitions

Fig. 2 presents the DSC thermograms of the 0-3 composites during the heating and cooling processes and for comparison, the DSC curves of the pure copolymer and TGS powder are also plotted. Both the Curie temperature

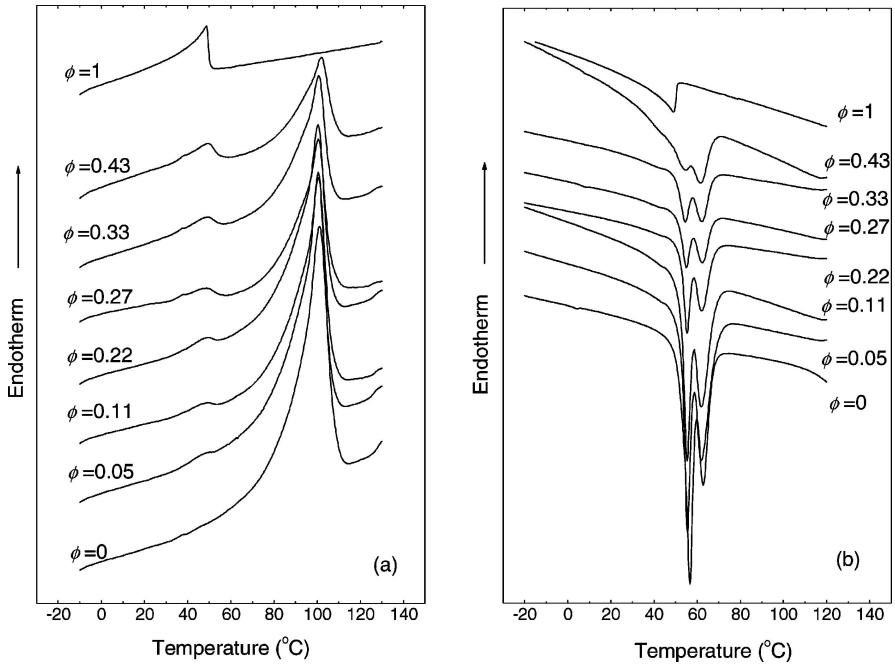

Figure 2 DSC thermograms of TGS/P(VDF-TrFE) 0-3 composites during the (a) heating and (b) cooling process.

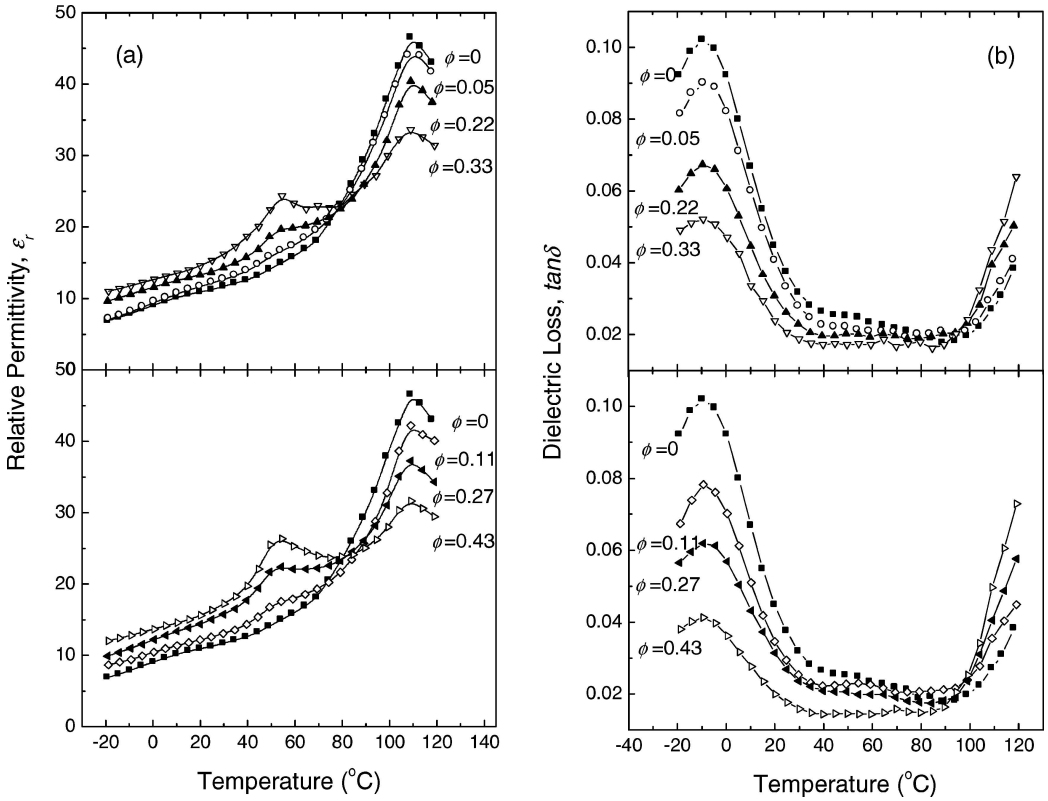

Figure 3 (a) Relative permittivity and (b) dielectric loss factor as a function of temperature for the unpoled TGS/P(VDF-TrFE) 0-3 composites measured at 10 kHz.

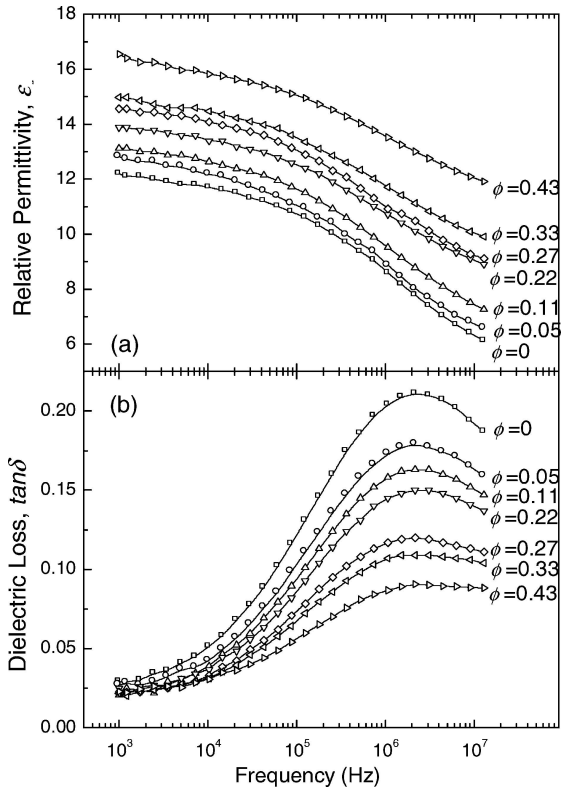

Figure 4 (a) Relative permittivity and (b) dielectric loss factor as a function of frequency for the unpoled TGS/P(VDF-TrFE) 0-3 composites measured at room temperature.

of TGS ($\phi = 1$) at 49°C and that of P(VDF-TrFE) ($\phi = 0$) at about 105°C (during heating) and 60°C (during cooling) appear in the DSC thermograms and the intensity of the endothermic/exothermic peaks follow the change in ϕ.

3.3. Dielectric permittivity

The temperature dependence of the relative permittivity ε_r and dielectric loss factor tan δ of the unpoled 0-3 composites measured at 10 kHz are presented in Fig. 3. The ferroelectric-paraelectric phase transition of TGS (at about 50°C) and P(VDF-TrFE) (at about 105°C) are both observed in the ε_r vs. temperature curves of the composites. The Curie point anomaly of TGS becomes more and more obvious as the TGS volume fraction increases. At the same time, the peak intensity corresponding to the phase transition of P(VDF-TrFE) copolymer decreases with increasing ϕ. In the tan δ vs temperature curves, a non-crystalline β relaxation of P(VDF-TrFE) is observed at about –10°C and the magnitude of the peak decreases gradually with increasing ϕ. In addition, there is a sharp rise of tan δ above 90°C in all samples presumably due to the Curie transition of the copolymer.

Fig. 4 shows the relative permittivity ε_r and dielectric loss factor tan δ as a function of frequency for the unpoled composites at room temperature. It is found that the dielectric behaviour of the 0-3 composites is dominated by the copolymer ($\phi = 0$). In the composites, the TGS phase possesses higher relative permittivity (the literature value of unpoled TGS single crystal along the b-axis [10] is $\varepsilon_r \sim$

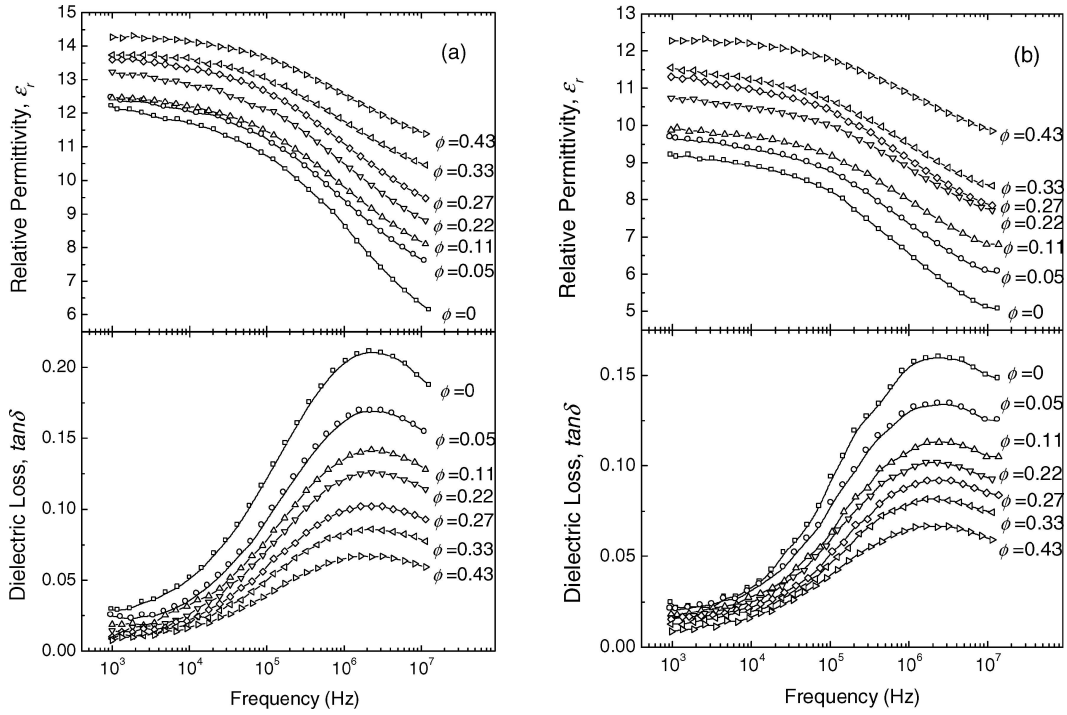

Figure 5 Relative permittivity and dielectric loss factor measured at room temperature as a function of frequency for (a) the composites with only the TGS phase poled and (b) with both phases poled.

38 at room temperature) than the P(VDF-TrFE) phase ($\varepsilon_r \sim 12$ for unpoled P(VDF-TrFE)), therefore ε_r increases with increasing ϕ. In the dielectric loss, the peak related to the β relaxation (at 2 MHz) of the copolymer is suppressed as the volume fraction of TGS increases. Fig. 5 shows the dielectric properties of the 0-3 composites as a function of frequency with only the TGS phase poled and with both phases poled. The variation of ε_r and tan δ in the poled composites with ϕ is similar to that of the unpoled samples (Fig. 4). The values of ε_r and tan δ for the samples with both phases poled are lower than those for the samples with only TGS poled, which are in turn lower than those of the unpoled samples due to the dipole alignment.

The relative permittivity of the composites can be understood in terms of the Bruggeman model [11]:

$$\left(\frac{\varepsilon_m}{\varepsilon}\right)^{1/3} = (1-\phi)\cdot\frac{\varepsilon_i - \varepsilon_m}{\varepsilon_i - \varepsilon} \qquad (2)$$

where ε, ε_i and ε_m represent the relative permittivity of the composite, the inclusion phase and the matrix phase, respectively. It should be noted that the relative permittivity of TGS powder is unknown and therefore the data for the copolymer and composites were least square fitted to the Bruggeman model. Fig. 6 shows the theoretical curves and experimental data for the unpoled samples, samples with only the TGS phase poled and samples with both phases poled. It can be seen that the theoretical values agree well with the experimental results with $\varepsilon_i \sim 20$ and $\varepsilon_i \sim 15$ for the unpoled and poled TGS powder, respectively. It is noted that $\varepsilon_r = 18.6$ as measured in a poled TGS single crystal supplied by the Institute of Crystal Materials, Shandong University, China.

3.4. Piezoelectric properties

Fig. 7 shows the piezoelectric coefficient d_{33} of the composites with only the TGS phase poled and the composites with both phases poled measured at room temperature. For the composites with only the TGS phase poled, the value of d_{33} increases from 0 to 15 pC/N when ϕ increases from 0 to 0.43. It should be noted that piezoelectric coefficients of P(VDF-TrFE) and TGS have opposite signs. Therefore, for the composites with both phases poled, d_{33} have neg-

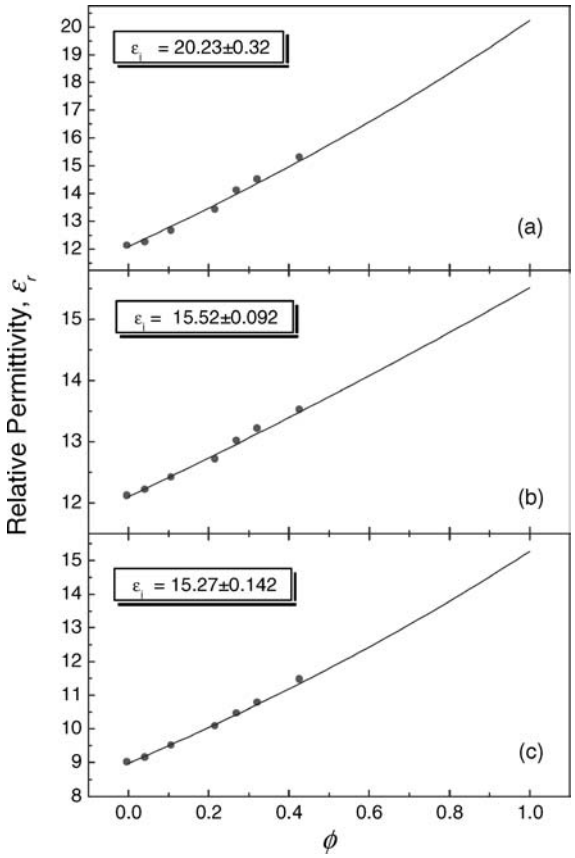

Figure 6 Relative permittivity as a function of ϕ for (a) the unpoled composites, (b) the composites with only the TGS phase poled and (c) the composites with both phases poled. The solid circles and lines represent the experimental data and Bruggeman model predictions, respectively.

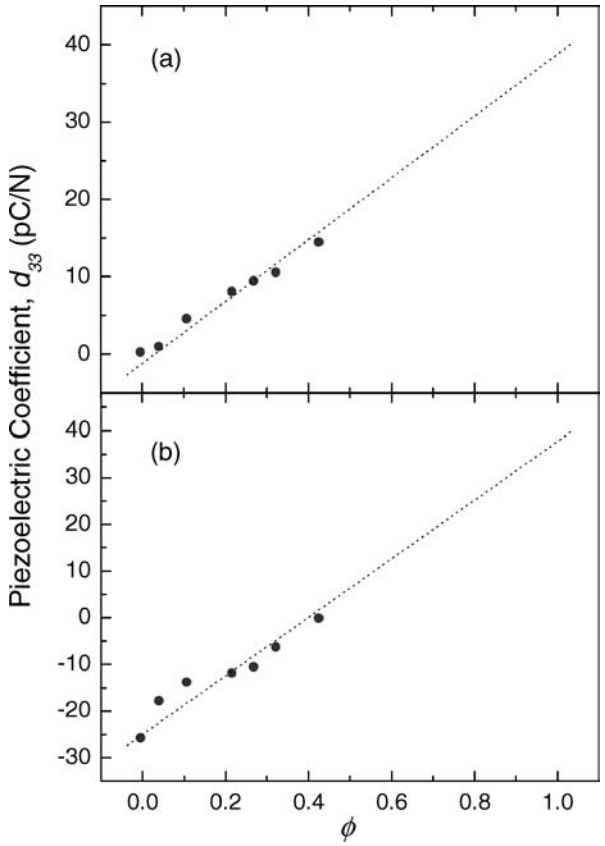

Figure 7 Piezoelectric coefficient measured at room temperature as a function of TGS volume fraction ϕ for the composites (a) with only the TGS phase poled and (b) with both phases poled. The dotted line is only a guide to the eye.

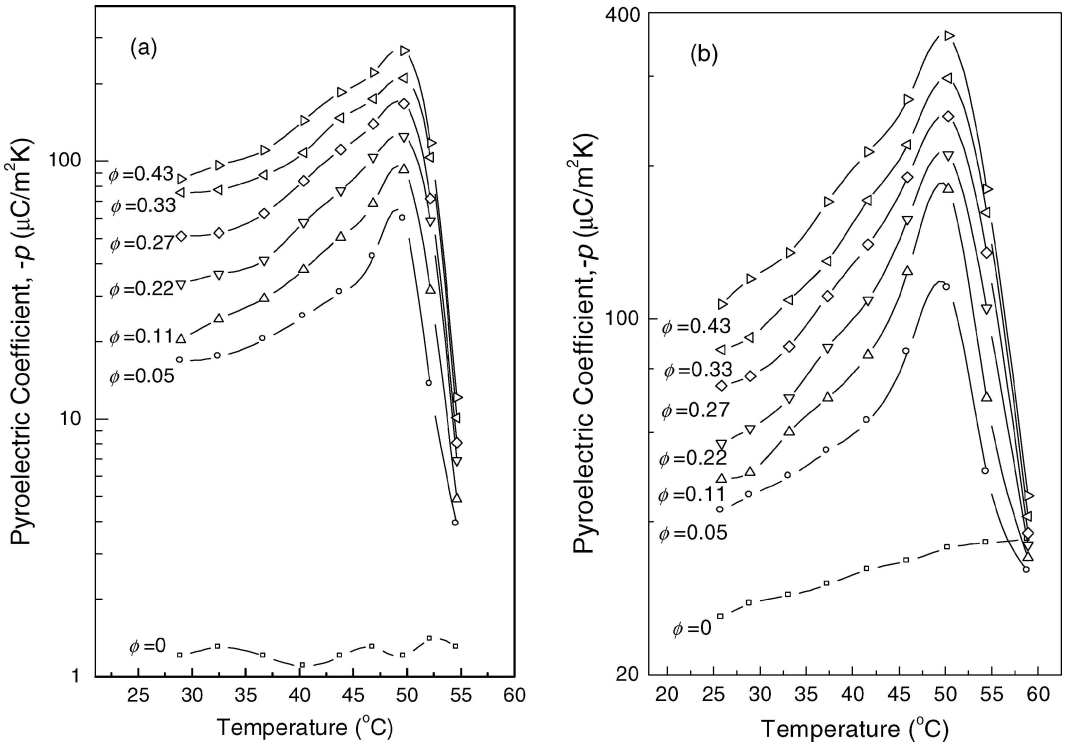

Figure 8 Pyroelectric coefficient as a function of temperature for the composites (a) with only the TGS phase poled and (b) with both phases poled.

ative values at low volume fraction of TGS mainly due to the contribution of the copolymer and as ϕ increases, d_{33} is reduced in magnitude and becomes nearly zero when $\phi = 0.43$. This $\phi = 0.43$ composite has the unique property that it is pyroelectric but non-piezoelectric. Vibration-induced noise can be minimized if this composite is used in fabricating pyroelectric sensors [12].

3.5. Pyroelectric properties

Fig. 8 shows the pyroelectric coefficients p of the 0-3 composites with only the TGS phase poled (Fig. 8a) and with both phases poled (Fig. 8b) as a function of temperature from room temperature to 60°C (above T_c of TGS). For comparison, the result of pure copolymer is also plotted in Fig. 8. The pyroelectric coefficient of the composites increases with increasing volume fraction of TGS. At any volume fraction of TGS, the pyroelectric coefficient of the composites increases with increasing temperature and reaches a maximum at about 50°C. Above the Curie transition of TGS, the magnitude of p decreases drastically because of the depolarization of TGS. The pyroelectric coefficient for the composites with only the TGS phase poled and the composites with both phases poled show similar temperature dependences and the magnitude of p for the samples with both phases poled is enhanced due to the contribution of the poled copolymer phase.

Using the effective-medium approach [6] (Equation 1), the effective pyroelectric coefficient p of the composites can be calculated. Fig. 9 shows the experimental results of the pyroelectric coefficients for composites with only the TGS phase poled and composites with two phases poled as a function of ϕ measured at room temperature. The theoretical curves are obtained by least square fitting of the data for the copolymer and composite samples to Equation 1. In the calculation, ε_m and p_m are measured values and ε and ε_i have been obtained using the Bruggeman model. It is seen that the experimental data and the theoretical calculation are in good agreement. The pyroelectric coefficient of the TGS powder obtained by the curve fitting is ~210 μC/m^{2}K which is lower than that measured using the poled TGS single crystal (p = 251 μC/m^{2}K).

There are several figures of merit (FOM) which describe the contribution of the physical properties of a material to the performance of a pyroelectric sensor. The current FOM F_i, voltage FOM F_V and detectivity FOM F_D are given by:

$$F_i = \frac{p}{c}; \quad F_V = \frac{p}{c\varepsilon_r\varepsilon_o}; \quad F_D = \frac{p}{c(\varepsilon_r\varepsilon_o \tan\delta)^{1/2}} \qquad (3)$$

where c is the heat capacity per unit volume (calculated from DSC thermograms). The figures of merit for composites with TGS phase poled and composites with two phases poled are calculated using the measured p, c, ε_r (at 1 kHz) and tan δ (at 1 kHz) at room temperature. The results are plotted in Fig. 10a (with only the

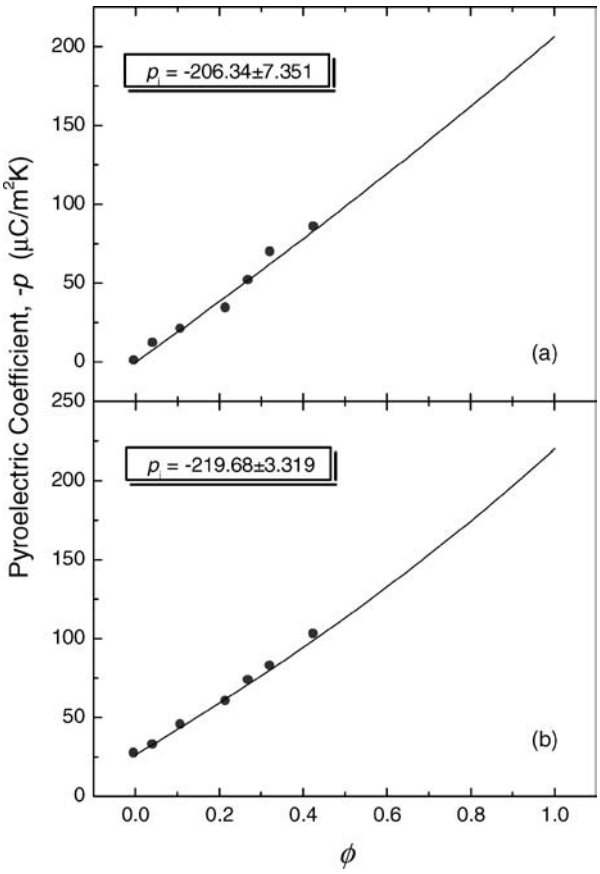

Figure 9 Pyroelectric coefficient as a function of ϕ for the composites (a) with only the TGS phase poled and (b) with both phases poled. The solid circles and lines represent the experimental data and effective medium model predictions, respectively.

TGS phase poled) and Fig. 10b (both phases poled). Compared to the values for the copolymer, all three FOM are improved in the composites, and the FOM values increase steadily with increasing ϕ. Tables I and II summarize the properties of the TGS/P(VDF-TrFE) 0-3 composites with only the TGS phase poled and the composites with both phases poled, respectively.

4. Conclusions

TGS/P(VDF-TrFE) 0-3 composites with various TGS volume fractions were fabricated by compression moulding. The composites were characterized by SEM and DSC. Three series of samples were prepared: unpoled composites, composites with only the TGS phase poled and composites with both phases poled. The dielectric, piezoelectric and pyroelectric properties of these samples were investigated. The relative permittivity and pyroelectric coefficient of the composites were found to increase with increasing TGS content. The relative permittivity and pyroelectric coefficient were compared with the theoretical predictions of the Bruggeman model and effective medium model, respectively, and good agreements have been obtained. It was also found that if the two phases were poled in the same direction, the pyroelectric contributions from TGS and P(VDF-TrFE) reinforced while piezoelectric contributions partially cancelled. Compared to the pure copolymer, the composites exhibited high pyroelectric coefficients and high pyroelectric figures of merit together with lower piezoelectric coefficients. The low piezoelectric activity is a significant advantage in pyroelectric sensor application since it will give rise to a low

TABLE I Properties of TGS/P(VDF-TrFE) 0-3 composites with the TGS phase poled

ϕ	c (MJ/m^3·K)	ε_r (1 kHz)	tan δ (1 kHZ)	d_{33} (pC/N)	$-p$ (μC/m^{2}K)	F_i (10^{-12}m/V)	F_V (m^2/C)	F_D (10^{-6}Pa$^{-1/2}$)
0	2.09	12.20	0.029	–	–	–	–	–
0.05	2.08	12.44	0.025	0.7	11.2	7.69	0.07	4.66
0.11	2.10	12.46	0.019	4.3	20.3	9.52	0.09	6.63
0.22	2.10	13.24	0.016	7.8	33.4	15.9	0.14	11.8
0.27	2.12	13.60	0.015	9.2	51.2	24.1	0.20	18.0
0.33	2.13	13.74	0.012	10.3	69.4	32.4	0.27	26.7
0.43	2.14	14.26	0.009	14.2	85.2	39.7	0.31	38.3
1[a]	2.18	18.6	0.004	40	251	115	0.70	142
1[b]	2.3	38	0.01	–	280	122	0.36	66

[a]Data obtained from the measurements of a poled TGS single crystal supplied by the Institute of Crystal Materials, Shandong University, China.
[b]From reference [10].

TABLE II Properties of TGS/P(VDF-TrFE) 0-3 composites with both phases poled

ϕ	c (MJ/m^3·K)	ε_r (1 kHz)	tan δ (1 kHZ)	d_{33} (pC/N)	$-$p (μC/m^{2}K)	F_i (10^{-12}m/V)	F_V (m^2/C)	F_D (10^{-6}Pa$^{-1/2}$)
0	2.09	9.20	0.024	−26.2	26.4	12.6	0.16	8.96
0.05	2.08	9.66	0.021	−18.2	32.3	15.5	0.18	11.6
0.11	2.10	9.87	0.018	−14.2	44.5	21.2	0.24	16.9
0.22	2.10	10.73	0.016	−12.3	59.5	28.3	0.30	22.8
0.27	2.12	11.31	0.011	−11.0	73.0	34.4	0.34	32.5
0.33	2.13	11.55	0.010	−6.7	82.6	38.8	0.38	37.3
0.43	2.14	12.27	0.008	−0.5	102	47.7	0.44	50.0

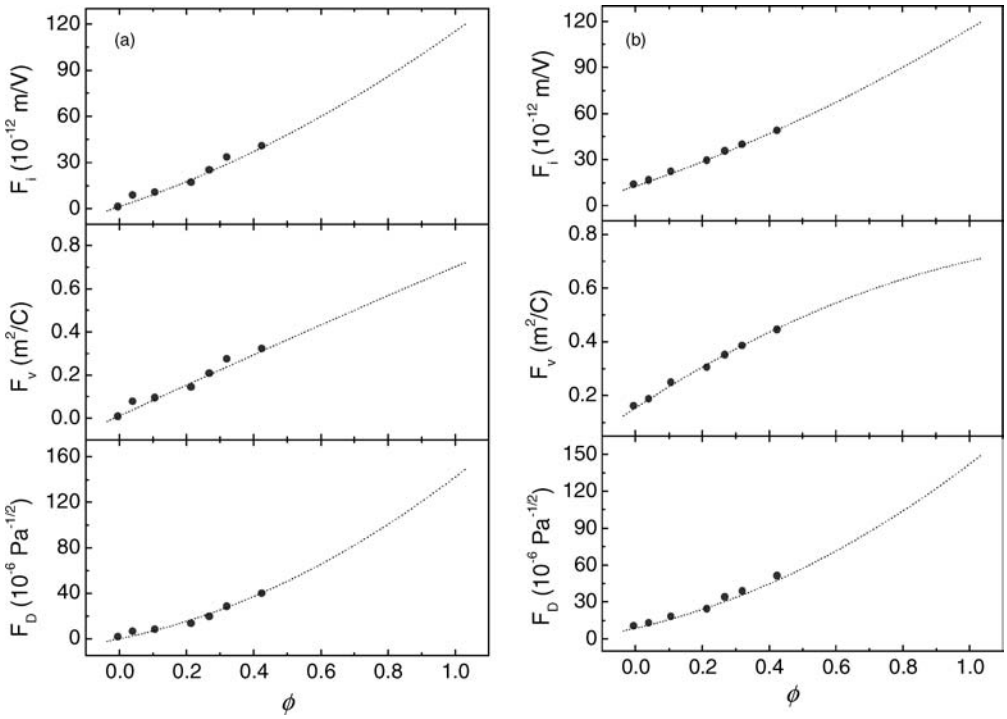

Figure 10 Room-temperature figures of merit F_i, F_V and F_D as a function of ϕ for the composites (a) with only the TGS phase poled and (b) with both phases poled.

vibration induced noise. Therefore, TGS/P(VDF-TrFE) 0-3 composite is a good candidate to be used as the sensing element for pyroelectric devices.

Acknowledgement

This work was supported by the Center for Smart Materials of the Hong Kong Polytechnic University.

References

1. C. DIAS and D. K. DAS-GUPTA, *IEEE Trans. Dielectr. Electr. Insul.* **3** (1996) 706.
2. T. YAMADA, T. UEDA and T. KITAYAMA, *J. Appl. Phys.* **53** (1982) 4328.
3. H. L. W. CHAN, W. K. CHAN, Y. ZHANG and C. L. CHOY, *IEEE Trans. Dielectr. Electr. Insul.* **5** (1998) 505.
4. H. L. W. CHAN, P. K. L. NG and C. L. CHOY, *Appl. Phys. Lett.* **74** (1999) 3029.
5. M. J. ABDULLAH and D. K. DAS-GUPTA, *IEEE Trans. Dielectr. Electr. Insul.* **25** (1990) 605.
6. K. H. CHEW, F. G. SHIN, B. PLOSS, H. L. W. CHAN and C. L. CHOY, *J. Appl. Phys.* **94** (2003) 1134.
7. Y. G. WANG, W. L. ZHONG and P. L. ZHANG, *ibid.* **74**, (1993) 521.
8. C. FANG, M. WANG and H. ZHOU, *Proc. 7 Intl. Sypm. Electrets (ISE 7)* (1991) 507.
9. B. PLOSS, B. PLOSS, F. G. SHIN, H. L. W. CHAN and C. L. CHOY, *Appl. Phys. Lett.* **76** (2000) 2776.
10. A. J. MOULSON and J. M. HERBERT, *Electroceramics: Materials, Properties, Applications* (John Wiley & Sons Press, 2003) p. 420.
11. D. A. G. BRUGGEMAN, *Ann. Phys. Lpz.* **24** (1935) 635.
12. B. PLOSS, W. M. FUNG, H. L.W. CHAN and C. L. CHOY, *Ferroelectrics* **263** (2001) 229